

Quantum illumination with noisy probes: Conditional advantages of non-Gaussianity

Rivu Gupta¹, Saptarshi Roy¹, Tamoghna Das², and Aditi Sen(De)¹

¹*Harish-Chandra Research Institute, HBNI, Chhatnag Road, Jhansi, Allahabad 211 019, India and*

²*International Centre for Theory of Quantum Technologies, University of Gdańsk, 80-952 Gdańsk, Poland.*

Entangled states like two-mode squeezed vacuum states are known to give quantum advantage in the illumination protocol, a method to detect a weakly reflecting target submerged in a thermal background. We use non-Gaussian photon-added and subtracted states as probes for the single shot quantum illumination both in the presence and absence of noise. Based on the difference between the Chernoff bounds obtained with the coherent state and the non-Gaussian state having equal signal strengths, whose positive values are referred to as a quantum advantage in illumination, we classify the performance of non-Gaussian states, when photons are added (subtracted) in (from) a single mode or in (from) both the modes. We highlight the hierarchy among Gaussian and non-Gaussian states obtained via this method, which is compatible with correlations per unit signal strength. Interestingly, such hierarchy is different when comparisons are made only using the Chernoff bounds. The entire analysis is performed in presence of different noisy apparatus like faulty twin-beam generator, imperfect photon addition or subtraction as well as with noisy non-Gaussian probe states.

I. INTRODUCTION

The non-classical features offered by quantum mechanics have revolutionized the development of modern technologies, ranging from computation [1–5], communication [6–12] to metrology and memory devices [13], far superior to their classical counterparts. Remarkable protocols like quantum teleportation [14–21], dense coding [22–29], quantum key distribution [30–34] boost the communication sector both with and without security while in the computational domain, algorithms based on quantum mechanics were discovered which offer as much as exponential speedup compared to the known methods in a classical computer [35–37]. The enhancing performance in most of the schemes rely on the amount of quantum correlations (QCs) present in the system, establishing them as the resource [38] for quantum advantage.

In the field of quantum metrology [39–43], illumination is the process to detect a target with low reflectivity encapsulated in a noisy thermal background [44–46]. In particular, a probe signal is sent towards the target and its presence or absence is inferred by analyzing the reflected beam. In quantum illumination (QI) [47–55], it was shown that the sensing capabilities of the target, modeled by a beam splitter (BS), can be improved by using entangled probes like two-mode squeezed vacuum (TMSV) state [56–60]. In this situation, one mode of the entangled pair is used as the signal mode, while the other mode (acting as idler) is directly sent to the detector to be stored and measured jointly after the signal mode reflected from the beam splitter returns (see Fig. 1 for schematics of the protocol). In this context, it was also shown that the initial shared entangled state between the signal and the idler modes still remains beneficial even in presence of loss and noise, which can destroy the resource [61–63]. Moreover, the idler mode needs to be stored until the time the signal returns which significantly reduces the range of QI since the storage of the idler for a longer duration is difficult [64]. For the classical illumination protocol using coherent states, homodyne detection turns out to be the optimal one [65] while for the Gaussian QI, more involved detection schemes are required to extract the quantum advantage, predicted theoretically [66–

74]. Finally, unlike other quantum devices, it is not yet clear whether quantum correlations, especially entanglement content of the initial Gaussian state is responsible for quantum advantage in the illumination process [59, 75–80].

On the other hand, it has been shown that non-Gaussian states, created by adding (subtracting) photons in (from) the TMSV states, which possess a higher amount of QCs than that of the Gaussian parent states, have potential to provide an advantage in the performance of QI [81–84] in a noiseless situation [67]. In this paper, we investigate the efficiency of non-Gaussian probe states in the presence of different kinds of noise or imperfections. The performance of QI is typically quantified by the minimum error probability for distinguishing the presence or absence of target states which is upper bounded by the quantum Chernoff bound (CB) [85–91]. In a noiseless scenario, we report a monotonic decrease of the CB with increasing number of added or subtracted photons from a single mode of the two-mode squeezed vacuum state. Symmetric two-mode operations (i.e., when equal number of photons are added or subtracted from both the modes) lowers the CB even further from the single mode value. We also observe that the non-Gaussian states can lower the CB even when the target reflectivity is very small and such an advantage increases with the number of photons added (subtracted). In a noisy situation, we find that the robustness in the CB against Gaussian noise which is admixed with the non-Gaussian states increases with the increase of non-Gaussianity. Similar trends can also be exhibited when the twin beam generator producing the parent TMSV state is faulty or when there is an imperfection in the photon addition and subtraction processes. According to the low values of Chernoff bounds, we can provide a hierarchy among the photon-added and -subtracted states which is quite similar to the QC present in these states (cf. [81, 82]).

We now refer a state to be quantum advantageous in the illumination protocol if the difference between the Chernoff bound of a coherent state and that of a given non-Gaussian state having the same signal strength is strictly positive. Based on it, we now classify different non-Gaussian states according to their performances in QI. We report that for low reflectivity, photon addition in the idler mode (or photon subtraction in the signal mode) and photon subtraction from both the modes

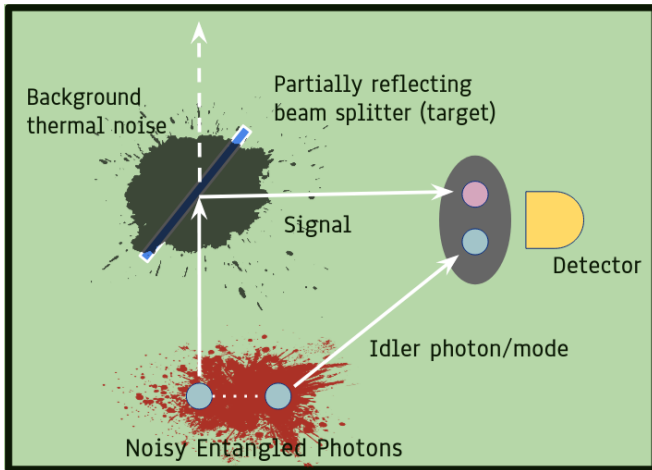


FIG. 1. A schematic representation of quantum illumination with noisy probes. The signal mode is sent towards the target, which is modeled by a weakly reflecting beam splitter. The idler mode is stored till the reflected signal comes back and the measurement is performed jointly on the two modes to infer the presence or absence of the target. The strong thermal background is always present, neighboring the target. Moreover, we consider different noise models in the probe states.

do yield quantum advantage while photon addition in both the modes or only in the signal mode cannot beat the classical limit, thereby giving non-positive difference. However, the hierarchy changes with the increase of the reflectivity of the BS. In a noisy scenario where the signal transmission line is assumed to be noisy, thereby affecting both non-Gaussian as well as coherent states, we, interestingly, observe that quantum advantage with non-Gaussian states increases even with the increase of noise upto a certain threshold value and then decreases as expected. Additionally, we arrive at a minimum operational efficiency of the photon addition (subtraction) apparatus to obtain quantum advantage which also takes care the probabilistic nature involved in the generation of non-Gaussian states from the TMSV states. This analysis also helps us to decide the most favorable resource, non-Gaussian or Gaussian, depending on the apparatus available. Note that although the entirety of the work focuses on advantage rendered by just a single copy of the probe state, the extension to QI with multiple copies is quite straightforward in our framework. Moreover, we report that the ranking of non-Gaussian states according to the advantage in the QI turns out to be in a good agreement with correlations quantified by mutual information and entanglement of the given state per signal photon.

The paper is organised in the following way. In Sec. II, we provide the prerequisites which include the Chernoff bound, the upper bound on the efficiency of the illumination protocol, its classical limit and the non-Gaussian states together with the noise models which we will use in our calculations. We also briefly describe our numerical methods. This is followed by Sec. III where we elucidate the advantages offered by non-Gaussian states, with particular focus on the comparison between the single-mode addition and subtraction of photons and the two mode operations. We then move on to the

definition of *quantum advantage* and show how only certain non-Gaussian states can actually outperform the classical protocol, while others fail to do so. At the end of section, we also deal with the illumination protocol in the situation of varying target reflectivity. In Sec. IV, we introduce noise in probe states, modeled by Gaussian local noise, faulty twin beam generators as well as imperfect non-Gaussian apparatus and we establish the robustness exhibited by non-Gaussian states to various noise models while in Sec. V, we compare Gaussian TMSV states with non-Gaussian states in two ways – one is when non-Gaussian apparatus is inefficient and another one is via correlation content of the states. We end our paper with the discussions of results in Sec. VI.

II. INGREDIENTS FOR ANALYZING QUANTUM ILLUMINATION WITH NON-GAUSSIAN RESOURCES

In this section, we discuss the tools required to analyze QI using non-Gaussian states both in presence and absence of noise. First, we present a brief primer about the non-Gaussian states to be used as probes for QI generated by photon addition and subtraction. We then describe the various components involved in the QI protocol. In particular, we specify the methodology to compute the performance of the QI protocol including numerical recipes used for evaluation. We then move on to present the various noise models that we employ to investigate noisy QI.

A. Non-Gaussian operations: Adding and subtracting photons

Non-Gaussianity has been proven to be performance enhancer in different contexts, ranging from entanglement [92, 93] to non-locality [94], and in the case of QI as well [81]. Among a plethora of de-Gaussification techniques, engineering non-Gaussian state via photon addition and subtraction offers the advantage of experimental realizability [95, 96] which, in turn, motivates us to take this route of de-Gaussification.

Before moving on to non-Gaussian resources, let us first consider the Gaussian two-mode squeezed vacuum state, given by

$$|\psi_r\rangle = \sum_{n=0}^{\infty} c_n |n, n\rangle, \quad (1)$$

where $c_n = (1-x)^{\frac{1}{2}} x^{\frac{n}{2}}$ with $x = \tanh^2 r$, r being the squeezing parameter and $\{|n\rangle\}$ representing the Fock basis.

By de-Gaussifying the TMSV state in both the modes (i.e., by adding k and l photons in the first and the second mode respectively), the (normalized) photon-added state can be represented as [92]

$$|\psi_r^{(k,l)}\rangle = \sum_{n=0}^{\infty} c_n^{(k,l)} |n+k, n+l\rangle, \quad (2)$$

where

$$c_n^{(k,l)} = \frac{x^{\frac{n}{2}}}{\sqrt{{}_2F_1(k+1, l+1, 1, x)}} \sqrt{\binom{n+k}{k} \binom{n+l}{l}}, \quad (3)$$

${}_2F_1$ is the Gauss Hypergeometric function, and $c_n^{(0,0)} = c_n$, while the photon-subtracted state obtained after subtracting photons from both the modes can be written as

$$|\psi_r^{(-k,-l)}\rangle = \sum_{n=\max\{k,l\}}^{\infty} c_n^{(-k,-l)} |n-k, n-l\rangle \quad (4)$$

with

$$c_n^{(-k,-l)} = \frac{x^{\frac{n-k}{2}}}{\sqrt{{}_2F_1(k+1, k+1, 1+k-l, x)}} \sqrt{\frac{\binom{n}{k} \binom{n}{l}}{\binom{k}{i}}}. \quad (5)$$

Without loss of generality, here we assume $k \geq l$. Notice, however, that Eq. (5) holds even for $l > k$ with k and l being interchanged in Gauss Hypergeometric function and in denominator.

Note. Instead of two modes, if addition (subtraction) is performed in a single mode, say, in the second mode, the corresponding output state can be obtained by putting $k = 0$, i.e.,

$$c_n^{(0,l)} = x^{\frac{n}{2}} (1-x)^{\frac{1+l}{2}} \sqrt{\binom{n+l}{l}}, \quad (6)$$

and in case of subtraction, it is

$$c_n^{(0,-l)} = x^{\frac{n-l}{2}} (1-x)^{\frac{1+l}{2}} \sqrt{\binom{n}{l}}. \quad (7)$$

Notice that here we consider the subtraction operation beyond $k \geq l$.

B. Elements of quantum illumination

The QI protocol comprises three main components – (i) the probes (signal and the idler), (ii) the weakly reflecting target embedded in a thermal background, and (iii) the detection scheme involving a joint measurement of the signal and the idler, as depicted schematically in Fig. 1. The task of inferring the presence or absence of the target reduces to a two state discrimination problem [89, 97–107] and hence, the performance of QI relies on the efficiency of the distinguishability protocol. The figure of merit of QI is then the minimum error probability that arises while discriminating the two non-orthogonal states, each of which corresponds to either of the two hypotheses: H_0 representing the scenario when the target is absent while H_1 identifying the presence of the target.

Mathematically, the weakly reflecting target is modelled by a beam splitter with a low reflectivity, κ . It is immersed in a thermal bath ρ_T , with mean photon number, N_B . The entangled probe used for QI is ρ_{IS} , where the subscript, I , is for

the idler and S represents the signal mode. When the target is present (hypothesis H_1), the reflected signal is admixed with the noise and the resultant state in the detector is given by

$$\text{Target present } (H_1) : \rho_1 = \text{Tr}_T(\hat{U}_{ST} \rho_{IS} \otimes \rho_T \hat{U}_{ST}^\dagger), \quad (8)$$

where \hat{U}_{ST} is the unitary representation of the BS acting on the signal and the thermal state, having the form $\hat{U}_{ST}(\xi) = \exp(\xi \hat{a}_S^\dagger \hat{a}_T - \xi^* \hat{a}_S \hat{a}_T^\dagger)$, with $\xi = \sin^{-1} \sqrt{\kappa}$. Here \hat{a}_S , \hat{a}_I , and \hat{a}_T are the annihilation operators for the signal, the idler, and the thermal modes respectively. For a very generic photon-added and -subtracted, TMSV state, as ρ_{IS} , Eq. (8) reduces to

$$\rho_1 = \sum_{n,n'=n_0}^{\infty} \sum_{m=0}^{\infty} \sum_{r=0}^{n \pm l} \sum_{s,s'=0}^m f(\{n\}, \{r\}, k, l, \kappa, N_B) |n \pm k, n + m \pm l - r - s\rangle \langle n' \pm k, n' + m \pm l - r - s|_{IS} \quad (9)$$

where the set $\{n\} = (n, n', m)$, $\{r\} = (r, s, s')$ and $n_0 = 0$ for addition and $n_0 = \max\{k, l\}$ for photon subtraction. The prefactor $f(\{n\}, \{r\}, k, l, \kappa, N_B)$ is given by

$$f = \frac{c_n^{\pm k, \pm l} c_{n'}^{\pm k, \pm l}}{\sqrt{(n \pm l)! (n' \pm l)!}} \frac{(N_B)^m}{(1 + N_B)^{1+m}} \frac{1}{m!} \binom{m}{s} \binom{m}{s'} (r + s)! \\ \binom{n \pm l}{r} \binom{n' \pm l}{r + s - s'} (-1)^{n+m-s+s'} \kappa^{\frac{1}{2}(n+n')-r+s' \pm l} \\ (1 - \kappa)^{m+r-s'} \sqrt{(n + m - r - s \pm l)! (n' + m - r - s \pm l)!} \quad (10)$$

where for the TMSV state, $k = l = 0$ and $\pm l$ and $\pm k$ represent photon addition and subtraction from the signal and idler modes respectively. The $c_n^{\pm k, \pm l}$ for various combinations of photonic operations are given in Eqs. (3), (5), (6), and (7).

Let us move to the hypothesis H_0 , i.e., when the signal is lost and the detector just gets the thermal state and the idler. In this case, the state simply takes the form as

$$\text{Target absent } (H_0) : \rho_0 = \text{Tr}_S \rho_{IS} \otimes \rho_T. \quad (11)$$

The explicit expression for ρ_0 reads as

$$\rho_0 = \sum_{n=n_0}^{\infty} \sum_{m=0}^{\infty} (c_n^{\pm k, \pm l})^2 \frac{N_B^m}{(1 + N_B)^{m+1}} |n \pm k, m\rangle \langle n \pm k, m|_{IT}, \quad (12)$$

where the lower limit n_0 of the first summation satisfies the same condition as for ρ_1 in Eq. (9) and the subscript I and T denote the idler and the mode of the thermal states respectively.

As mentioned before, the efficiency of QI reduces to the problem of effectively distinguishing ρ_0 from ρ_1 , or multiple copies of them with the least possible error using an optimal measurement scheme. Assuming that there is a priori equal probability of the target being present or absent, the minimum error probability for distinguishing $\rho_0^{\otimes M}$ and $\rho_1^{\otimes M}$ can then be expressed as [44]

$$P_M = \frac{1}{2} \left(1 - \frac{1}{2} \|\rho_0^{\otimes M} - \rho_1^{\otimes M}\|_1 \right), \quad (13)$$

where $\|X\|_1 = \text{tr}|X|$ represents the trace norm [49, 81, 82, 108]. From the above expression, it is not easy to calculate the error probability, and hence we will focus on the upper bound of it, the quantum Chernoff bound [85–91], given by

$$P_M \leq \frac{1}{2} Q^M. \quad (14)$$

where

$$Q = \min_{0 \leq \alpha \leq 1} \text{tr} [\rho_0^\alpha \rho_1^{1-\alpha}]. \quad (15)$$

Note that the Chernoff bound for M copies is just the M^{th} power of the Chernoff bound for a single copy. Moreover, since the quantum CB is asymptotically tight [89, 91], the single-copy bound dictates the hierarchies of error probabilities obtained in the large M -case. We, therefore, throughout the manuscript, work with the single shot case, i.e., for $M = 1$. Results for any finite M can simply be obtained from Eq. (14).

C. The classical limit

The scheme [44, 49, 88, 109] which uses coherent states, $|\sqrt{N_S}\rangle$, as signal probe for illumination can be referred as classical illumination method. The single-shot Chernoff bound for the same is computed to be

$$Q_c = e^{-\kappa N_S (\sqrt{N_B} - \sqrt{N_B+1})^2}, \quad (16)$$

which in the limit $N_B \gg 1$ reduces to

$$Q_c \approx e^{-\frac{\kappa N_S}{4N_B}}. \quad (17)$$

The corresponding minimum error probability for M -copies of the coherent state is then upper bounded by

$$P_M^c \leq \frac{1}{2} Q_c^M. \quad (18)$$

In this paper, when we observe $P_M < P_M^c$, where average number of photons in the signal probe is fixed to N_S in both the cases under comparison, we claim that quantum advantage is obtained in the QI method.

D. Noise models for probes

To analyse the case of noisy illumination protocol, we induce certain types of imperfections in the probe states. We enlist them now.

1. Local noise in probes

We consider two-mode entangled states in the presence of local noise, acting independently on each mode. The noise

model which we consider, yields the mixed state (see ref. [94]), given by

$$\rho = (1-p)|\psi\rangle\langle\psi| + p \left(\sum_{n=0}^{\infty} \mu_n |n\rangle\langle n| \otimes \sum_{m=0}^{\infty} \nu_m |m\rangle\langle m| \right) \quad (19)$$

where $|\psi\rangle$ denotes the non-Gaussian entangled state, and $\sum_{n=0}^{\infty} \mu_n = \sum_{m=0}^{\infty} \nu_m = 1$. In our analysis, μ_n and ν_m are taken to have a Gaussian form, with

$$\begin{aligned} \mu_n &= \frac{2}{1 + \vartheta_3(0, e^{-\sigma_1^{-2}})} e^{-n^2/\sigma_1^2}, \\ \text{and } \nu_m &= \frac{2}{1 + \vartheta_3(0, e^{-\sigma_2^{-2}})} e^{-m^2/\sigma_2^2}. \end{aligned} \quad (20)$$

Here, σ_1 and σ_2 are the chosen noise parameters which control the average number of photons in either mode of the noise part, and ϑ_3 is the Jacobi theta function [110] of order 3. Throughout our analysis, we set $\sigma_1 = \sigma_2 = 1$. The results remain qualitatively similar with other choices of σ_i , as long as they are not too high to erase the quantum advantage.

2. Faulty generation of two-mode state

Another inefficiency during the production of probes can occur when the twin beam generator making the TMSV state is faulty [94]. As a result, the probe state has less squeezing than actually expected. Therefore, the protocol may be designed for a squeezing parameter r but the actual resource may have less efficiency due to a lower squeezing parameter $r' (< r)$ which in turn translates to $x' (< x)$. Thus the performance obtained may not be optimal and there may even be a situation when there is no advantage at all, over the blind guess. We explore the role of non-Gaussianity in this respect, to figure out whether quantum advantage can be increased or even restored through the application of photon-added or -subtracted states in this scenario.

3. Imperfect photon addition and subtraction

Due to several imperfections, e.g., dark counts of the detector [111–113], the probe states produced may not have the desired number of added or subtracted photons. As a result, the final state is a mixture of states with varying levels of non-Gaussianity. We assume that, for a given number k of photons to be added or subtracted, the state is mixed with other states having $k, k-1, k-2, \dots, k-m$ ($m \leq k$) added or subtracted photons, with different probabilities. Here, m represents the cutoff in the discrepancy which can be incorporated due to the imperfect creation process. The state, therefore, takes the form as

$$\tilde{\rho}_{\pm k} = \sum_{i=0}^m p_i \rho_{\pm|k-i|}. \quad (21)$$

We will be interested to compute the performance of QI using $\tilde{\rho}_{\pm k}$ and compare it with the corresponding classical bound.

E. Method for computing Chernoff bounds:

Let us discuss the method which we use to calculate the Chernoff bounds for non-Gaussian states. The density matrices corresponding to ρ_1 and ρ_0 are constructed according to Eqs. (9) and (12). The truncated infinity, i.e., N in the summation is chosen in such a way, that the tolerance in trace and the computed CB is less than 10^{-8} . Under such conditions, the matrices have dimension $(N \pm k + 1)(2N \pm l + 1) \times (N \pm k + 1)(2N \pm l + 1)$, where $(N \pm k + 1) \times (N \pm k + 1)$ denotes the size of the idler subsystem and $(2N \pm l + 1) \times (2N \pm l + 1)$ is that for the signal subsystem, with $+$ and $-$ representing the photon addition and subtraction respectively. In case of the TMSV state, and the photon-added states, it is observed that any $N \geq 35$ is sufficient while for photon subtraction, we have to take $N \geq 45$. In case of mixed states, as defined in Eqs. (19) and (28), convergence is achieved for the same limits. Thereafter, we optimise Eq. (14) over α to obtain the Chernoff bound. All the calculations are performed for a fixed value of κ , N_B and x with k and l running from 0 to 10. In most of our analysis, we set $\kappa = 0.01$, representing the target reflectivity, unless mentioned otherwise and the mean number of photons in the thermal background is taken to be unity. A major part of our calculations are done by setting $x = 0.2$ and 0.05 .

Remark: An error probability of 0.5 is trivial and any deviation from the same may be considered as enhancement of performance. In the entirety of our analysis, we consider any difference which is $\leq 10^{-4}$ to be negligible and thus a Chernoff bound ≥ 0.4999 is rounded off to be 0.5. Throughout our work, we represent states with photons added in one mode as ‘‘sPA’’, and those with photons added in both the modes as ‘‘PA’’ while photon subtracted states are dubbed as ‘‘PS’’. Interestingly, states with photons added in the signal mode behave exactly similar to those with subtracted photons from the idler mode and vice versa [94]. Thus, we deal only with single mode addition of photons and the performance of probes with subtracted photons from one mode follows trivially.

III. NON-GAUSSIAN QUANTUM ILLUMINATION

It has already been established that the introduction of non-Gaussianity in the resource state through photon addition and subtraction can generate high amount of quantum correlations. Hence there is a possibility that these classes of states can lead to a lower error probability, in terms of CB in the illumination protocol, than that of the coherent state. The indication in this direction was obtained by taking examples of photon-added and -subtracted states [81, 82].

We here analyze the performance of QI via computing the Chernoff bound into two situations – (1) single mode operations which include adding photons in either the idler or the signal mode; (2) when addition and subtraction are performed in both the modes. Moreover, we study the effects of variation of target reflectivity on the performance of quantum illumina-

tion.

A. Single mode operations: Signal vs. Idler

Let us add photons in the single mode of the TMSV as specified by the coefficients in Eqs. (6) and (7) and compute the QI performance. As mentioned before, QI scheme with subtracting photons from a single mode is already included in the results for photon addition. For example, we know $|\psi_r^{(k,0)}\rangle = |\psi_r^{(0,-k)}\rangle$. Let us specify the behavior of Chernoff bound, \mathcal{Q} , under single mode operations.

1. *Monotonicity.* \mathcal{Q} decreases monotonically with the number of added photons, n , both in the idler and the signal modes as shown in Fig. 2 with $x = 0.05$ and $x = 0.2$. Interestingly, owing to the low squeezing at $x = 0.05$, the error probability for the TMSV state cannot go below 0.5 although non-Gaussian states are successful in doing so. However, later we will address whether such decrements really imply the advantage in QI or not.
2. *Asymmetry.* Although the CB behaves monotonically with the added number of photons in a single mode, it depends on the mode, (signal or idler), in which the photons are added. In particular, photons added in the idler mode always gives a poorer detection probability than the case when photons are added in the signal mode of the entangled state. The effect becomes prominent with the addition of higher number of photons, thereby inducing more non-Gaussianity in the state, see Fig. 2.

Note. For measures like entanglement (E), there is a symmetry between the modes, and we have $E(|\psi_r^{(k,0)}\rangle) = E(|\psi_r^{(0,k)}\rangle)$. However, for CB, in case of single mode photonic operations, $\mathcal{Q}(|\psi_r^{(k,0)}\rangle) < \mathcal{Q}(|\psi_r^{(0,k)}\rangle)$ and hence there is an asymmetry inherent in its definition. Therefore, for photon subtraction, we get a reversed relation compared to that of addition, i.e., subtraction of photons from the idler mode induces lower CB than that of the photon subtraction from the signal mode and hence we have $\mathcal{Q}(|\psi_r^{(-k,0)}\rangle) > \mathcal{Q}(|\psi_r^{(0,-k)}\rangle)$.

B. Two mode operations: Addition vs. subtraction

We now address two main questions pertaining to photonic operations – (1) whether single mode operations are better than two-mode operations; (2) whether addition in both the modes is better than subtraction in terms of lowering CB. Let us first examine the first question. When an equal n number of photons are added in both the modes of the TMSV, we get lower CB compared to the single mode operations, with the symmetric combination yielding the best performance. However, surprisingly when photons are subtracted from both the

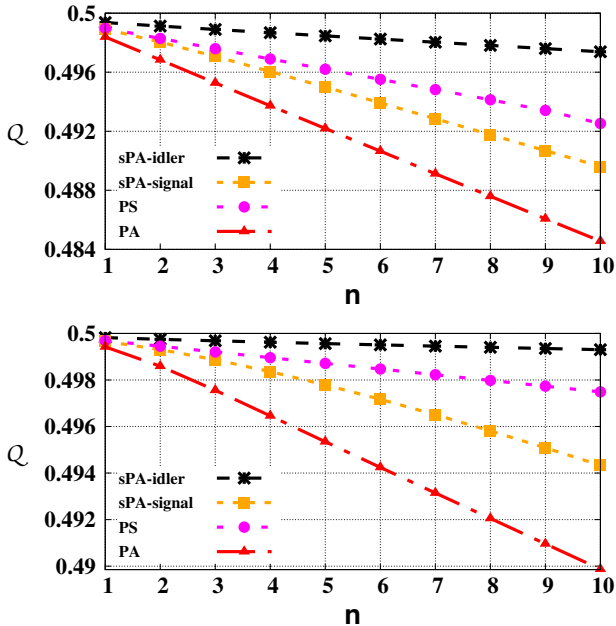


FIG. 2. (Color Online.) Chernoff bound, Q , (ordinate) against number of photons added (subtracted), n , (abscissa) to create different non-Gaussian states from TMSV. Stars and squares are for the states with photons added either in the idler mode, denoted by sPA-idler and signal mode (sPA-signal) respectively while circles and triangles represent states when n number of photons are added (PA) and subtracted (PS) from both the modes. Notice that Q for sPA-idler and sPA-signal are equal to that of photon-subtracted state from the signal mode and idler modes respectively. The squeezing parameter is set to $x = 0.2$ for the upper panel and $x = 0.05$ for the lower panel. All the axes and dimensionless.

modes, it actually gives higher CB over the single mode operations. In particular, it implies that subtraction of photons from the idler (i.e., addition in the signal) is better in terms of lowering CB than subtracting equal number of photons from both the modes, irrespective of x , as shown in Fig. 2.

Secondly, we compare the CB between photon addition and subtraction. The computation of CB shows that photon addition in both the modes gives lower CB than that of the photon-subtracted states and the difference increases with the increase of n . Moreover, adding photons in the signal mode (similarly, subtracting photons in the idler mode) leads to low CB compared to that of the subtraction from both the modes. Notice, however, that among all the non-Gaussian states, the states with photons added in both the modes can give the lowest CB, although it does not lead to an advantage in QI, which will be discussed in the subsequent section.

C. Does reduction in Chernoff bound ensure quantum advantage in QI?

The analysis upto now shows the benefit of non-Gaussianity in terms of an ubiquitous decrease in CB, when more photons are added or subtracted from the TMSV. If CB reduction does

translate into quantum advantage, then one can conclude that the non-Gaussian photon-added and -subtracted states show better performance than the parent TMSV (cf. [81, 82]). Note that such a comparison scheme may be considered natural and intuitive since it follows the same strategy when considering enhancements of entanglement [92, 93], violations of Bell inequalities [94] etc.

Moreover, we know that photon addition and subtraction can be considered as a sort of distillation procedure where fewer number of higher entangled states are obtained from a large number of low entangled states, and hence for entanglement, content, such comparison is perfect. However, for schemes like quantum illumination where higher number of copies are involved, reduction of copies via distillation must be associated to the performance-calibration scheme, which we will consider in a subsequent section. Hence comparing identical number of copies of Gaussian and non-Gaussian states does not lead to a fair conclusion. If they are done, they must be considered as independent states and the comparison must be made by fixing one relevant physical quantity, which, in case of QI, is the signal strength [81].

Let us set up a more appropriate scheme to assess quantum advantage for QI. Under the more realistic method of comparison, the hierarchy of states gets altered and sometimes, the non-Gaussian states which provided low CB fail to provide any quantum advantage. Therefore, the central question that we want to address, under the new comparison methods, is *when does non-Gaussianity provide quantum advantage in illumination?*

The quantum advantage in QI for the TMSV state is defined by the difference between the Chernoff bounds for the TMSV state and that of the coherent state with identical intensity in the signal mode. In a similar fashion, *quantum advantage for the photon-added or -subtracted states* can be defined as the difference between the Chernoff bounds for the non-Gaussian states and the coherent state for a fixed signal strength. In this case, for a given photon-added (-subtracted) state, $|\psi_r^{(\pm k, \pm l)}\rangle$, we first compute the average number of photons it possesses in its signal mode, which reads as

$$N_S = \sum_{n=\frac{k-(\pm k)}{2}}^{\infty} (n \pm k) |c_n^{(\pm k, \pm l)}|^2. \quad (22)$$

The classical limit is then found by using the coherent state which has the same signal strength as in $|\psi_r^{(\pm k, \pm l)}\rangle$, i.e., $N_S(|\psi_r^{(\pm k, \pm l)}\rangle)$. In particular, for a given N_S , we track the gap between the single shot quantum Chernoff bounds for the state $|\psi_r^{(\pm k, \pm l)}\rangle$ and the corresponding coherent state with the same signal strength. Mathematically, we are interested in the quantity, which we call quantum advantage in quantum illumination, given by

$$\Delta(|\psi_r^{(\pm k, \pm l)}\rangle) = Q_c - Q(|\psi_r^{(\pm k, \pm l)}\rangle), \quad (23)$$

where Q_c can be computed from Eq. (16) using the same signal strength, N_S , as obtained from Eq. (22). If $\Delta(|\psi_r^{(\pm k, \pm l)}\rangle) > 0$, we report a quantum advantage in QI, while $\Delta(|\psi_r^{(\pm k, \pm l)}\rangle) \leq 0$ implies that the classical protocol

outperforms or performs in a similar fashion as the QI scheme, for the given quantum probe ρ_{IS} .

D. Classification of non-Gaussian states according to their performance in quantum illumination

We are now going to classify the non-Gaussian states according to this figure of merit, Δ . We observe that Δ is positive for the state with photons subtracted state from both the modes, thereby establishing quantum advantage in QI while the states with photons added in the idler mode (i.e., photon subtracted from the signal mode) also prove to be a good resource for illumination according to Δ (see Fig. 3). Our results indicate that in order to obtain quantum advantage from non-Gaussian operations, it is favorable to perform photon subtraction, either from the signal mode or from both the modes. Furthermore, photon-subtraction being easier experimentally, [114] adds to the importance of our result.

As it is evident from Fig. 3, all non-Gaussian states, having N_S equal to the classical signal, do not perform equally well. In particular, the non-Gaussian states with photons added only in the signal as well as in both the modes, cannot surpass the classical limit which is clearly visible from the negative values of Δ .

Note 1. The same hierarchies will be maintained for higher number of copies of the probe states used for QI which directly follows from Eq. (14).

Note 2. Such a definition of quantum advantage also has limitations. In particular, it ignores the probabilistic nature of the photon addition (subtraction) operation in (from) the TMSV state.

Note 3. In presence of low reflectivity, TMSV is found to be better than the corresponding photon-added and -subtracted states, having the same signal strength [115]. To match the signal strength for both the states, the squeezing parameter of the TMSV, turns out to be higher. This feature is not unique to QI, but also happens in case of entanglement as well, where for a given average number photons, the TMSV state gives the maximal amount of entanglement [81] over any photon-added (- subtracted) state.

E. Quantum advantage by varying target reflectivity

In QI protocol, as described in Sec. II, a weakly reflecting target is modelled by a beam splitter of low reflectivity. Now, the detection scheme may have to cater to various targets having different reflectivities κ . If κ is low, the efficiency of the protocol always decreases. In this context, it is interesting to find the trade-off between the low reflectivity and the enhancement of QI due to non-Gaussianity. In case of the TMSV state, we find that for $\kappa \leq 0.001$, there is no advantage over the blind guesses of the target, while non-Gaussian states can still provide a better detection probability \mathcal{Q} even for such a low reflectivity as illustrated in Fig. 4.

For low reflectivity, even the state with photons added only in the idler mode is unable to provide low CB unless the added

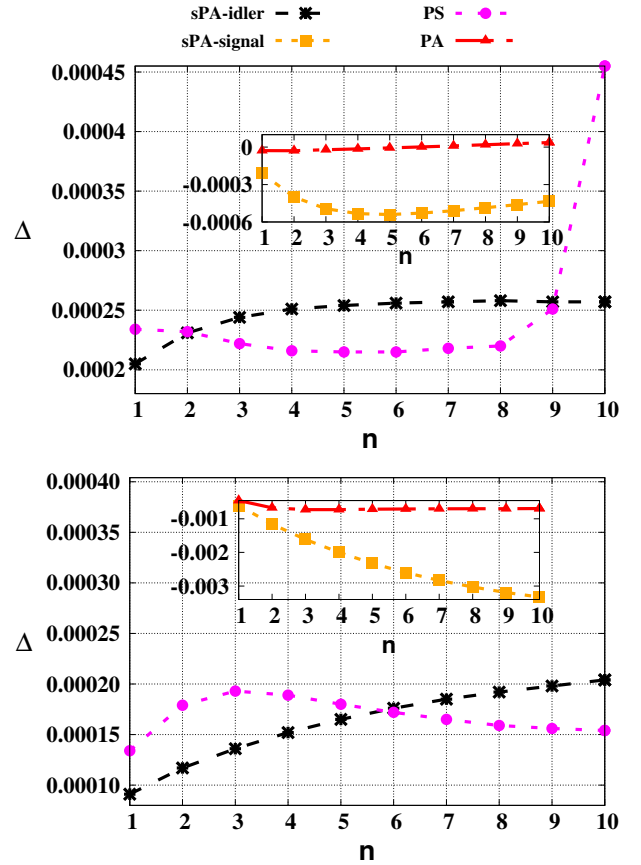


FIG. 3. (Color Online.) Quantum advantage in the illumination protocol, Δ defined in Eq. (23), (vertical axis) vs. n (horizontal axis). All other specifications are same as in Fig. 2. Both the axes are dimensionless.

number of photons is $n \geq 4$. However, similar to previous scenarios, single photon addition (subtraction) from the signal (idler) mode incorporates enough non-Gaussianity to have a low value of CB. The hierarchy of the non-Gaussian states in terms of lower error probability is maintained such that photon subtracted states perform better than states with photons added in the idler but cannot overpower states with photons added in the signal mode.

Effect of varying target reflectivity on quantum efficiency. For a fixed number of photons added (subtracted), we now compare Δ obtained from different non-Gaussian states by varying κ . For reflectivities of the order of 10^{-2} or higher, addition of photons in the idler mode, and in both the modes as well as subtraction of photons from both the modes can outperform the classical protocol, thereby demonstrating the quantum advantage (see Fig. 5 where number of photons added (subtracted) in (from) a single or both the modes is 5). However, the states having photons added in the signal mode (subtracted from the idler mode) can never give $\Delta > 0$ and thus, it is not suitable as a probe state. Notice, however, that for extremely low reflectivity, $\kappa < 10^{-2}$, neither the TMSV state nor the non-Gaussian states can provide any quantum advantage, thereby showing the coherent state-based protocol to

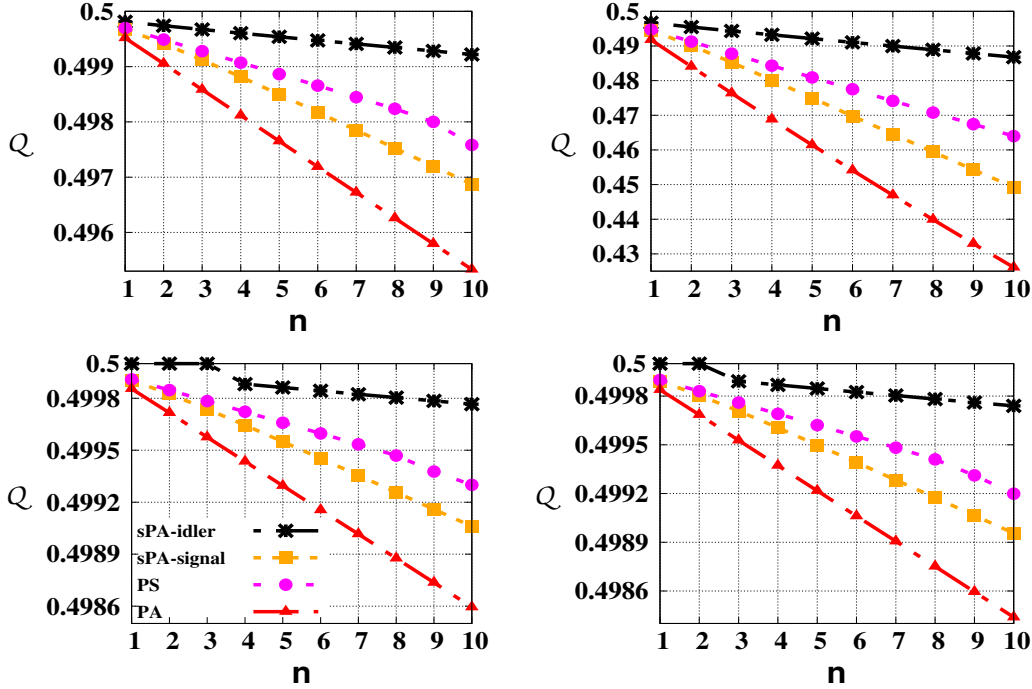


FIG. 4. (Color Online.) Performance of Chernoff bound (y -axis) with respect to n (x -axis) by varying reflectivity, κ . (Upper panel) $\kappa = 0.0009$ on the left and $\kappa = 0.001$ on the right. (Lower panel, left) $\kappa = 0.003$ and (right) $\kappa = 0.05$. The TMSV state from which non-Gaussian states are created has $x = 0.2$. All other specifications are same as in Fig. 2. Both the axes are dimensionless.

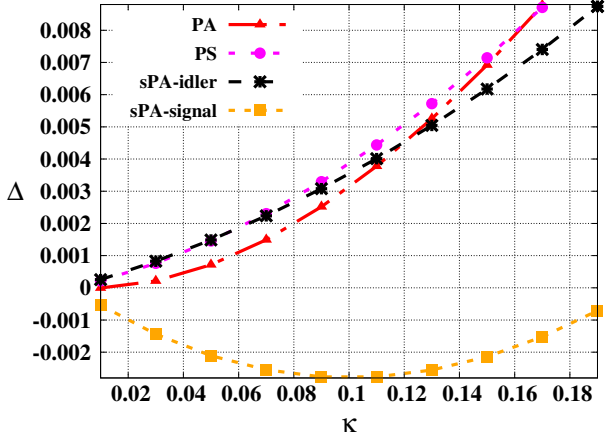


FIG. 5. (Color Online.) Δ (ordinate) vs. κ (abscissa). Here $n = 5$. All other specifications are same as in Fig. 2. Both the axes are dimensionless.

be good for a single-shot case.

IV. CHERNOFF BOUND VS. QUANTUM ADVANTAGE IN ILLUMINATION WITH NOISY NON-GAUSSIAN PROBES

In this section, we consider the performance of entangled states in presence of different kinds of noise in resource states, as discussed in Sec. II D. Till now, noise is considered as a

strong thermal background, present around the target. Here, we focus on a situation when the two-mode photon-added and -subtracted entangled states, admixed with i) local noise, ii) generated via faulty twin beam generator, iii) having imperfect photon addition or subtraction, are used as a probe. We investigate the behavior of CB as well as quantum advantage in QI, defined in Eq. (23), for these noisy probes. In spite of the worsening performance in QI in presence of noise, we report several advantages exclusive to non-Gaussianity such as robustness against noise in QI and activation of quantum advantage in CB.

A. Chernoff bound against local noise in non-Gaussian states

Let us first consider the local noise models given in Eqs. (19) and (20). The robustness against noise is characterized by the maximum value of the mixing probability, $p = p^*$, in Eq. (19) below which CB is lower than 0.5 (upto numerical accuracy of the order of 10^{-4}). Before moving to the photon-added and -subtracted states, let us first notice that for the TMSV state, p^* turns out to be 0.5 when $x = 0.2$ while it reduces to 0.4 for low squeezing strengths, $x = 0.05$.

1. Enhanced robustness against noise

As photons are added or subtracted from a single mode, either from the signal or from the idler, we denote, the maximal

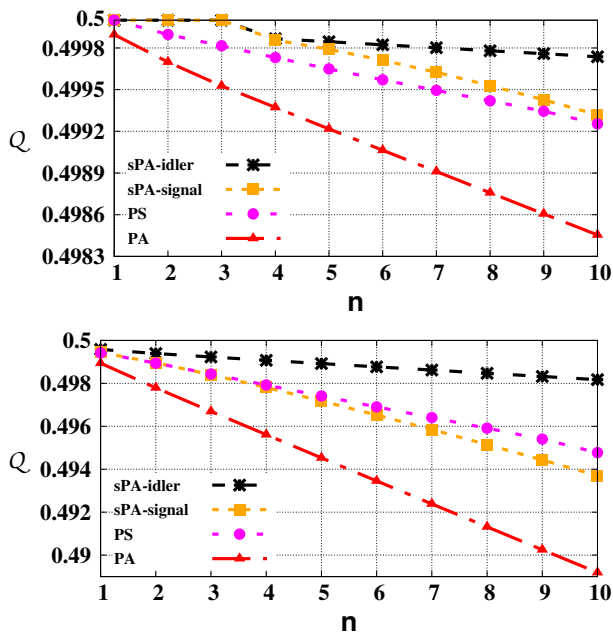


FIG. 6. (Color Online.) Robustness and activation of CB against noise. \mathcal{Q} (vertical axis) with respect to n (horizontal axis) when probes are mixed with local Gaussian noise, given in Eq. (19). The upper panel represents states with $p = 0.9$ (which shows activation of Chernoff bound in case of addition of photons in the idler or signal mode) while the lower panel corresponds to $p = 0.3$. Here $x = 0.2$. All other specifications are same as in Fig. 2. Both the axes are dimensionless.

amount of noise, for which the error probability is $\mathcal{Q} < 0.5$, as p^* . An increasing value of p^* , indicates *enhanced robustness to noise*, see Fig. 6. We illustrate our results for two exemplary squeezing parameters, x , although the results remain qualitatively similar for other squeezing parameters:

1. For $x = 0.2$, when photons are added or subtracted in the signal or in the idler, p^* increases to 0.7 from 0.5, indicating an enhanced robustness. When more photons are added (subtracted) in a single mode, and when two mode operations have been employed, p^* increases further.
2. Such robustness decreases with the decrease of squeezing parameter of the original TMSV state used for non-Gaussian operations. For example, when $x = 0.05$, the tolerance against noise increases for single mode operations, increasing $p^* = 0.6$ from $p^* = 0.4$ in the TMSV Gaussian state from which non-Gaussian states are created, i.e., $p_{nG}^* > p_{TMSV}^*$. The trend is more prominent when photons are added (subtracted) in both the modes.

Note. Since μ_n and ν_m represent the number of photons in each mode of the noise, if they increase, so does the average number of noisy photons, and thus the performance of CB becomes poor. In case of the Gaussian noise model, the mean number of noisy photons increases with an increase of σ_1 and σ_2 in Eq. (20), thereby providing higher error probability with the increase of noise.

2. Activation of Chernoff bound via non-Gaussianity

Another interesting feature of non-Gaussianity is that, for noise strengths that undermine the performance of the TMSV state such that it is not better than blindly guessing the target, photon-added and -subtracted states give a reasonable CB (which is much below than 0.5). It means that the non-Gaussianity can help to counter the adverse effect of noise and lead to activation of \mathcal{Q} . For example, with $x = 0.05$, for local noise, TMSV state cannot outperform the blind guess probability, $p = 0.5$, while the states with photons added in the idler mode, show activation for $n \geq 3$ (see Fig. 6 (upper panel)) and with $x = 0.2$, $n \geq 2$ is enough.

B. Quantum advantage with noisy non-Gaussian probes

In presence of Gaussian noise, we find that the quantum advantage in terms of positive Δ cannot not be achieved using the photon-added and -subtracted states if the noiseless coherent and noisy non-Gaussian states possess the same signal strength. Specifically, in this scenario, $\Delta(\rho) \leq 0$.

Instead of comparing the performance of noisy non-Gaussian states with the optimal classical scheme by coherent states, let us consider a scenario where the signal transmission line itself is affected by noise and hence any state passing through it suffers from same amount of noise, i.e., noisy channel affects both coherent and photon-added (subtracted) states. When local Gaussian noise acts on it, a coherent state, transforms in the following way:

$$\rho = (1-p)|\omega\rangle\langle\omega| + p \sum_{n=0}^{\infty} \mu_n |n\rangle\langle n| \quad (24)$$

where $|\omega\rangle = e^{-\frac{1}{2}|\omega|^2} \sum_{n=0}^{\infty} \frac{\omega^n}{\sqrt{n!}} |n\rangle\langle n|$ is the coherent state and μ_n is given in Eq. (20). The signal strength is then given by

$$N_S = (1-p)|\omega|^2 + p \sum_{n=0}^{\infty} n\mu_n. \quad (25)$$

When the target is present, the state ρ_1 (as in Eq. (8)) reads

$$\rho_1 = e^{-|\omega|^2} \sum_{n,n'=0}^{\infty} \sum_{m=0}^{\infty} \sum_{r=0}^n \sum_{s,s'=0}^m f(\{n\}, \{r\}, \kappa, N_B) |n+m-r-s\rangle\langle n'+m-r-s|_S \quad (26)$$

where $f(\{n\}, \{r\}, \kappa, N_B)$ has the same form as Eq. (10) with $k = l = 0$ and $c_n = \frac{\omega^n}{\sqrt{n!}}$. Since the coherent state constitutes a single mode probe, in the absence of the target, the signal is lost and all that the detector receives is the background thermal noise i.e., $\rho_0 = \rho_T$. We evaluate the Chernoff bound for the noisy coherent state using these expressions.

We compare now the noisy non-Gaussian states with the corresponding noisy coherent state, i.e., noise effects both non-Gaussian and coherent states in a similar fashion, so that the signal strength gets modified in exactly the same way as in

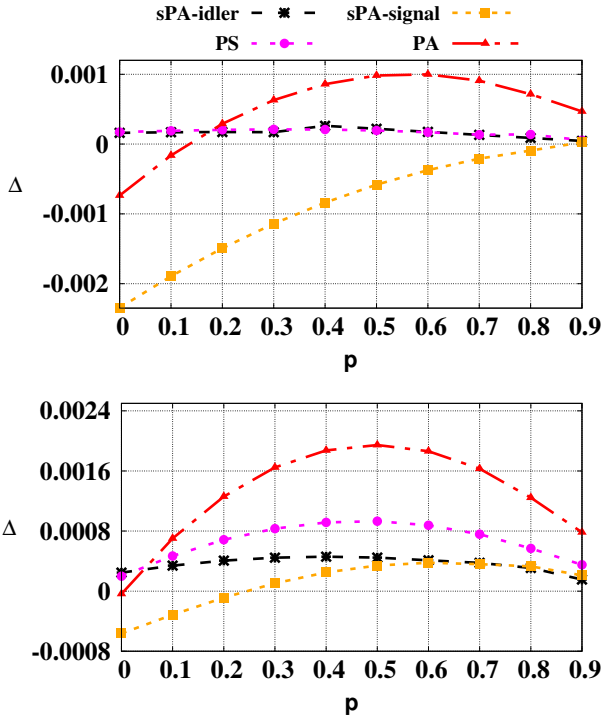


FIG. 7. (Color Online.) Robustness of quantum advantage, Δ , (ordinate) with the variation of noise strength, p (abscissa). In Gaussian noise, $\sigma_1 = \sigma_2 = 1$. In all cases, the number of photons added or subtracted is set to be 5. We fix $x = 0.2$ in the lower panel and $x = 0.05$ in the upper panel. All other notations are same as in Fig. 3. Both the axes are dimensionless.

Eq. (25). For the comparison under the same signal strength, the choice of the intensity of the coherent light can be chosen using Eqs. (25) and (22) by

$$|\omega|^2 = \sum_{n=\frac{k-(\pm k)}{2}}^{\infty} (n \pm k) |c_n^{(\pm k, \pm l)}|^2 \quad (27)$$

which is nothing but the signal strength of the entangled mixed state given in Eq. (19). It is evident from Fig. 7 that $\Delta > 0$ for all non-Gaussian states for a certain range of p . This is due to the fact that with the increase of noise, the classical resource is much more affected by the noise and hence its performance degrades drastically. However, at low levels of noise, the state with photons added in the signal mode performs poorly as compared to the classical probe (as shown in Fig. 7 where Δ of this state becomes positive when $p \geq 0.3$, from the negative value in presence of low noise). With the increase of the noise strength, all the non-Gaussian resources perform much better than that of the classical probe until the noise probability becomes too large (≥ 0.5) and Δ starts to decrease again, although remaining positive. Thus we demonstrate that under the destructive effect of noise, the non-Gaussian probes are more robust than the noisy classical probes having the same signal strength, thereby exhibiting quantum advantage. In this scenario, the state with photons added in both the modes constitutes the most robust resource. The results remain qualita-

tively similar even when the squeezing strength, x is moderately small.

C. Effects of faulty twin beam generator on quantum efficiency

As described in Sec. IID2, we consider the effects of faulty twin beam generator which produces TMSV with $x' < x$ (where x is the promised squeezing strength) on CB. Notice that a similar investigation can be carried out with $x' > x$ which we are not considering since states with higher squeezing are typically hard to prepare compared to those with lower one. The Chernoff bound for the non-Gaussian states is calculated for squeezing parameter x , thereby yielding α_x as its optimal parameter. However, due to faulty twin beam generator, we obtain the TMSV state having squeezing x' which we are unaware of. Hence during computation of CB, we apply optimal α_x in Eq. (15), instead of $\alpha_{x'}$, thereby leading to a higher error probability compared to that obtained via x . We refer it as \tilde{Q} . Notice here that CB increases, with the decrease of x of TMSV, thereby increasing the probability of error.

We now consider a non-Gaussian state with squeezing x' and show that it can offer a lower \tilde{Q} , i.e., a better detection probability, even with an inefficient protocol. Specifically, for a fixed x , the minimum error probability of discriminating targets, quantified by \tilde{Q} increases with the increase in the difference between x and x' .

For $x = 0.05$, in our analysis, we obtain that CB decreases for all non-Gaussian states irrespective of the number of photons added (subtracted), provided $x - x' \leq 0.035$, as shown in Fig. 9. On the other hand, when $x - x'$, increases and it is ≥ 0.035 , we observed that \tilde{Q} almost remains fixed to 0.5, even for a moderate number of photons added in the idler mode, thereby showing no improvement in error probability with non-Gaussianity.

Quantum advantage due to faulty twin beam generator. For this analysis, let us fix $x = 0.05$ and choose various values of $x' < x$. Here we consider coherent states with N_S corresponding to x , since x' is an artefact of the faulty device and beyond the scope of the experimentalist. As illustrated in Fig. 9, in presence of low faulty twin-beam generator, i.e. when $x - x' < 0.03$, the positivity of Δ guarantees the quantum advantage by the photon-subtracted and the photon-added states in the idler mode while addition of photons in both the modes and in the signal modes fail to show any advantage. The beneficial nature of non-Gaussian states disappears with the slight increase of $x - x'$. Notice also that the results remain similar for other values of squeezing parameter.

D. Condition for quantum advantage with imperfect photon addition or subtraction

Let us demonstrate the case when the photonic operations are imperfect, and non-Gaussianity still continues to provide improvements in QI. To demonstrate it, we consider imperfect subtraction of photons with $k = l = 2$ and $m \leq 2$,

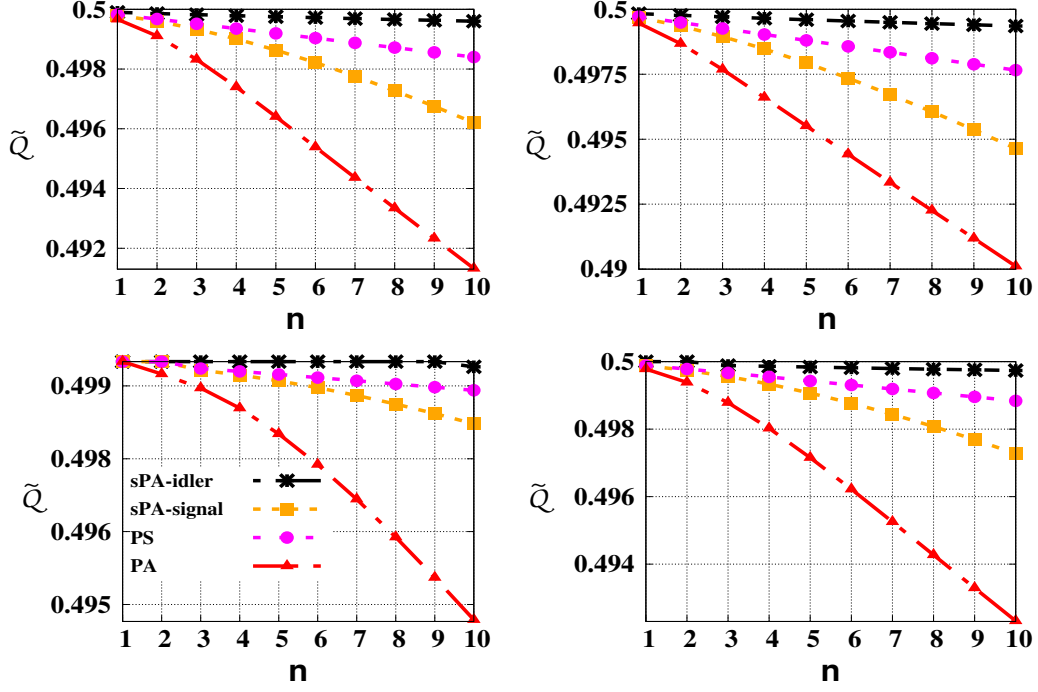


FIG. 8. (Color Online.) Effects of faulty twin beam generator on \tilde{Q} (y -axis) vs. n (x -axis). In all the figures, $x = 0.05$. (Upper panel (left)) $x' = 0.025$, (right) $x' = 0.045$. (Lower panel (left)) $x' = 0.005$ and on right, $x' = 0.015$. All other legends are same as in previous figures. Both the axes are dimensionless.

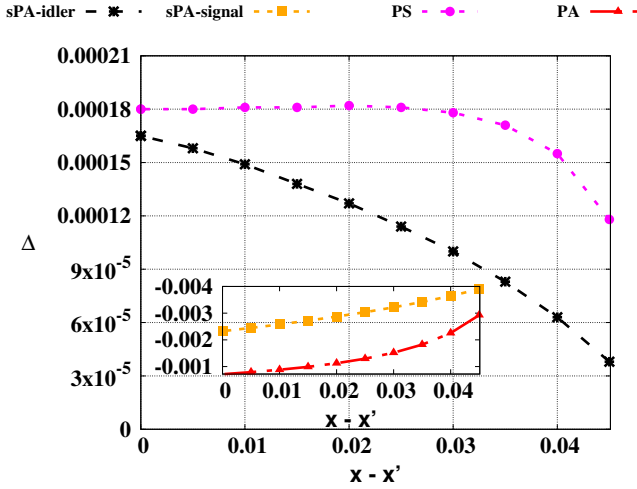


FIG. 9. (Color Online.) Role of faulty twin beam generator on the performance of illumination. Quantum advantage, Δ , (vertical axis) against $x - x'$ (horizontal axis). All other specifications are same as in Fig. 3. Both the axes are dimensionless.

in accordance with Sec. IID3. Thus we have a two photon subtracted state, mixed with a single photon subtracted state and the Gaussian TMSV state as the probe in the illumination scheme which reads as

$$\tilde{\rho} = p\rho_2 + p'\rho_1 + p''\rho_{TMSV} \quad (28)$$

with $p + p' + p'' = 1$. Here ρ_i represents the state where i th number of photons have been subtracted from both signal and the idler modes.

It is seen that, even with imperfect probe generation, the CB is always lower than that with the Gaussian state, i.e., $\mathcal{Q}(\tilde{\rho}) > \mathcal{Q}(\rho_{TMSV})$. We consider three probabilities, p —corresponding to the perfect two photon subtracted state, p' —for the single photon subtracted state and p'' —for the TMSV state respectively. For our investigation, we set a fixed value of p'' and vary p , with p' being determined by the normalization condition in Eq. (28). As the probability of obtaining the required state decreases, the CB monotonically increases, as is evident from the bottom panel in Fig. 10. Moreover, we notice that as long as the desired perfect state has $p \geq p''$, the CB possess a lower value than that obtained for the photon-added state in a single mode. Therefore, even if the required non-Gaussian state is obtained with a very small probability, its mere presence is enough to ensure a low error probability for discriminating targets.

Deterioration of the performance of QI under imperfection. Comparing the performance of non-Gaussian states with that of a coherent state having the same signal strength, we find that even if the photon subtraction mechanism is imperfect, the resulting state can always beat the classical limit, as depicted in the top panel of Fig. 10 by the positive values of Δ . However, such states can never perform better than the perfect two photon- and a single photon-subtracted states. As the probability, p'' of generating the TMSV state, due to the imperfection of the apparatus, increases, the illumination efficiency falls considerably, thereby implying that even a highly

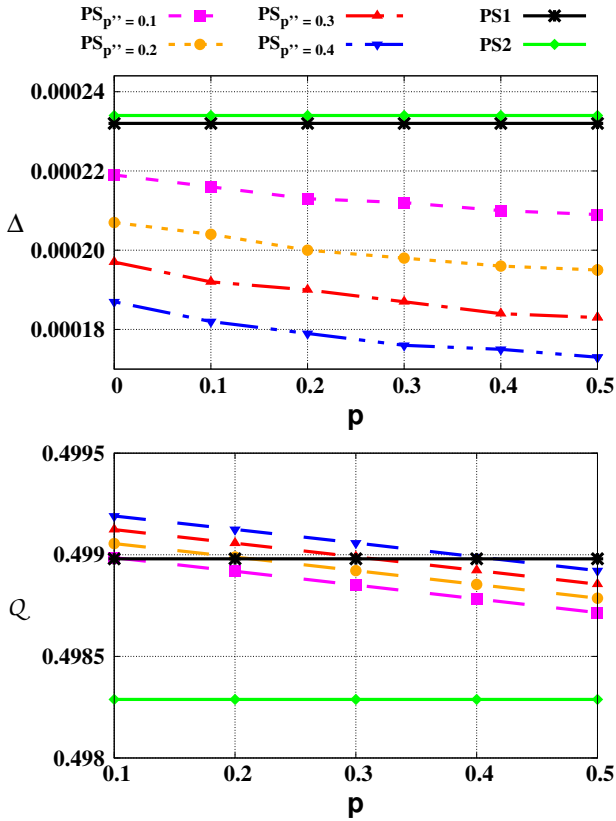


FIG. 10. (Color Online.) Consequence of imperfect photon subtraction device on illumination. (Upper panel) Quantum advantage (Δ) (ordinate) against p (abscissa) while (lower panel) Q vs. p . Stars and diamond represent the states without imperfection, i.e., photon-subtracted state from a single mode and subtraction of photons from both the modes respectively. The imperfect states given in Eq. (28) are for $p'' = 0.1$ (squares), $p'' = 0.2$ (upward triangles), $p'' = 0.3$ (circles) and $p'' = 0.4$ (downward triangles). Both the axes are dimensionless.

imperfect photon subtraction protocol can yield substantial quantum advantage. Our results indicate that photon subtraction is an efficient process to obtain quantum advantage over the coherent state even if the state generation process is not perfectly optimal. Notice that in case of photon addition, such an advantage cannot be seen.

V. PROBABILISTIC IMPROVEMENTS VIA NON-GAUSSIANITY

In this section, we employ another procedure to compare the efficiency of QI method by Gaussian and non-Gaussian states. In particular, we consider the indefiniteness involved in the photon addition and subtraction operations in which a fewer number of non-Gaussian states are distilled from a higher number of TMSV states. This is different from the imperfection in the photon addition (subtraction) mechanism (Sec. IV D), as we will discuss shortly. Our comparison scheme in the first subsection takes into account of the in-

determinacy in the photon addition and subtraction process, both in presence and absence of noise. Moreover, we compute bipartite entanglement and mutual information towards identifying the physical properties responsible for obtaining quantum gain in illumination.

A. Inefficient non-Gaussian apparatus

Photon addition and subtraction are not deterministic processes (cf. [92] and references therein). Due to inefficiency of the non-Gaussian protocol, the desired photon-added or -subtracted state may be produced only with a certain probability. This means that to produce M' copies of a non-Gaussian state, we need M copies of the TMSV resource, with $M > M'$. Therefore, it can be argued that comparing the QI performance of photon-added or -subtracted states with the same number of TMSV states is incorrect (unless they are treated as independent states and the comparison is made under fixed signal strength). If the overall efficiency of the photonic operation is η , then we have $M' = \eta M$ copies of a non-Gaussian state having started with M copies of the TMSV state. Note that the probability η can be interpreted as the efficiency of the apparatus implementing a particular photonic operation. Hence the correct comparison has to be made between M copies of the TMSV and $M' = \eta M$ copies of the non-Gaussian state. In this section, we try to illustrate that, even if the apparatus is not a 100% efficient in preparing photon-added and -subtracted states, non-Gaussianity can offer added advantage in the illumination protocol, as compared to the TMSV states' performance. In particular, we find out the minimum efficiency η required to extract quantum advantage. This analysis is different from that of imperfect addition (subtraction) of photons discussed before. In case of imperfect non-Gaussian mechanism, a mixed state is always produced, which has states with varying number of added (subtracted) photons with different probabilities. However, in case of inefficient non-Gaussian protocol, we always obtain a pure state as the probe, albeit with a probability η which is less than unity.

The main idea is to find the minimum number of non-Gaussian states (M'), which can outperform M copies of the TMSV state. Equivalently, we are able to calculate the minimum probability of success (η) of the non-Gaussian apparatus. As mentioned before, we now try to find the minimum efficiency which the non-Gaussian apparatus must have, so that, on obtaining a less number of output states, we can beat the protocol of a greater number of input Gaussian states. In that case, instead of using M copies of the TMSV state, we can feed them to the apparatus, thereby receiving ηM copies of the photon-added (-subtracted) state, and then use these probes for a more efficient illumination protocol. This illustrates the power of non-Gaussianity, where a smaller number of non-Gaussian states can help to achieve better error probability of target detection, in contrast to the TMSV states.

To calculate the minimum efficiency required by the apparatus, so that quantum advantage is achieved over the TMSV state, we compute the minimum value of η which satisfies the

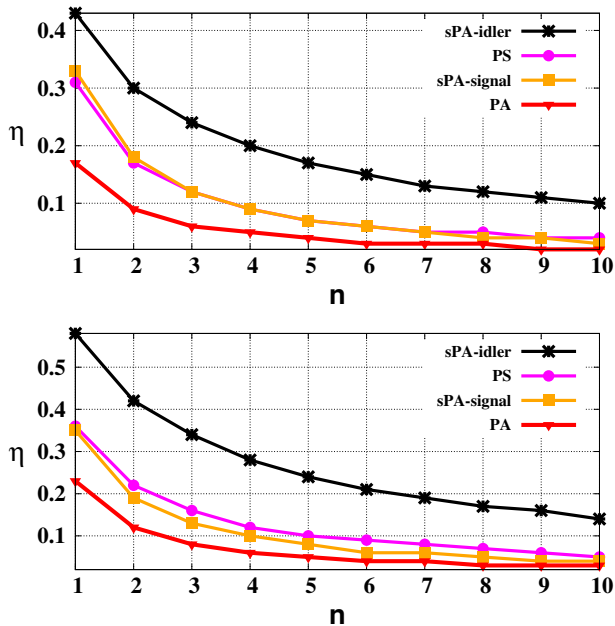


FIG. 11. (Color Online.) Minimum operational efficiency (η) required (ordinate) to create states with n added (subtracted) photons (abscissa) which can outperform a higher number of Gaussian states with ($x = 0.2$), given in Eq. (29). (Upper panel) The probes are noisy mixed states with $p = 0.3$ and Gaussian noise parameters $\sigma_1 = \sigma_2 = 1$ in Eq. (19). (Lower panel) The probes are pure non-Gaussian states. All other symbols used here are same as in Fig. 2. Both the axes are dimensionless.

following:

$$(\mathcal{Q}_{opt})_{TMSV}^M = (\mathcal{Q}_{opt})_{non-Gaussian}^{\eta M} \quad (29)$$

where \mathcal{Q}_{opt} is the Chernoff bound in Eq. (14). When the photonic operation fails, which does with a probability of $1 - \eta$, we are left with a junk state which is useless for any information processing purpose.

Our results indicate that the minimum operational efficiency required by the non-Gaussian apparatus, decreases with the increase in the number of photons added or subtracted. This is also consistent with experiments, since it is more difficult to introduce higher non-Gaussianity in a state (see Fig. 11). It turns out that addition of photons to the idler mode demands the most efficiency while subtraction of photons from both the modes succeeds the former type of states, followed by addition of photons in the signal mode. Thus instead of subtracting photons from both the modes, we can deal with addition of the same to the signal mode to obtain a low CB.

1. Enhancement of robustness against noise

We now try to address whether the enhancement features of non-Gaussianity obtained in the case where TMSV was admixed with local Gaussian noise in Sec. IV A, persist when

the indeterministic nature of photonic operations are considered while calibrating the performance of QI.

Let us illustrate this via an example. Consider a noisy TMSV state of the form in Eq. (19) with $x = 0.2$ and $p = 0.3$. In this configuration, the TMSV continues to provide $\mathcal{Q}_{opt} < 0.5$. When photons are added or subtracted probabilistically, we report in Fig. 11, the minimum efficiency required for such a process to decrease \mathcal{Q}_{opt} over the TMSV value. Interestingly, we can observe that the non-Gaussian states can beat the TMSV state with even less efficiency of production when inherent noise is present in the probe states compared to the noiseless scenario. Therefore, in the presence of local Gaussian noise, *there is an improvement in decreasing error probability in presence of non-Gaussianity over the noiseless case.*

2. Probabilistic activation of quantum advantage

Like activation reported in Sec. IV A 2, we now investigate the possibility of activation when the probabilistic nature of photonic operations is considered. To do that, we again consider the noisy TMSV state as in Eq. (19) with $x = 0.2$, but this time with $p > p^* = 0.5$. The choice $p > p^*$ ensures that the noisy TMSV state does not provide any advantage in decreasing CB.

Interestingly, since the initial state from which non-Gaussian states are produced is useless for quantum illumination, and our analysis in Sec. IV A 2 suggests that non-Gaussian states corresponding to the parent TMSV state are beneficial, we clearly see that we can obtain probabilistic activation of quantum advantage for any non-zero efficiency of the photonic operations. The probability of getting a “useful” state for QI from the initial “useless” TMSV state is equal to the efficiency of the photon addition (subtraction) process. Our analysis clearly demonstrates how updating the interpretation of quantum advantage changes the nature of the enhancements obtained in QI.

B. Role of correlations on quantum illumination

We now investigate the role of correlations between the two modes of the probe state on the illumination protocol – mutual information (MI) [116–118] which is defined as $MI = S(\rho_A) + S(\rho_B) - S(\rho_{AB})$ for a two-mode state ρ_{AB} where $S(\rho)$ denotes the von-Neumann entropy of a quantum state, and entanglement present per signal photon in the probe states. In our analysis, entanglement for mixed state is quantified via logarithmic negativity [119, 120], defined as $LN = \log_2(2N(\rho_{AB}) + 1)$, where $N(\rho_{AB})$, known as *negativity*, is the sum of absolute value of the negative eigenvalues of the partial transposed version ρ_{AB}^{TA} of the two-mode state. Let us carry out the investigation for the noisy probes as specified by Eq. (19).

We find that the Gaussian TMSV state possess the maximum amount of correlation, both in terms of MI/N_s and LN/N_s as depicted in Fig. 12. This may be an indication

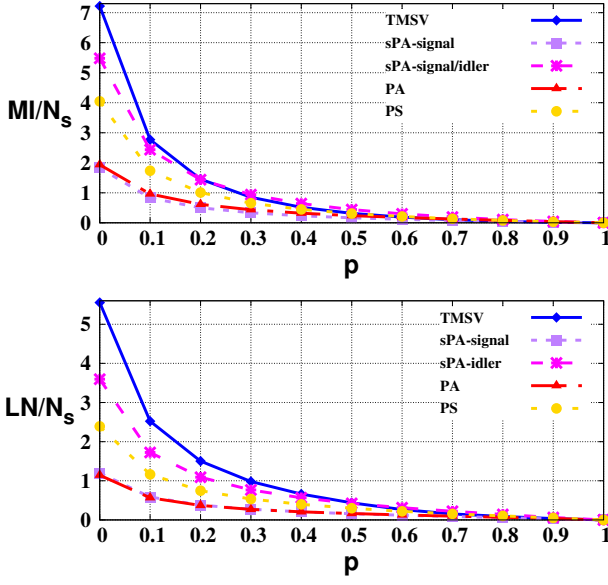


FIG. 12. (Color Online.) Correlations per signal photon (ordinate) against Gaussian noise strength, p . (Upper panel) Mutual information (MI) and (lower panel) logarithmic negativity. Diamonds correspond to TMSV states and other legends are same as in Fig. 2. For all non-Gaussian states, the number of added (subtracted) photons in each mode is $n = 5$.

of such a state being the optimal probe for the illumination purposes [81]. Interestingly, among the non-Gaussian states, the states with photon added in the idler and the ones with photons subtracted from both the modes have higher correlation with respect to p per signal photon than that of the states having photon addition in signal and in both the modes. Specifically, non-Gaussian states which cannot furnish any quantum advantage over coherent states having the same N_S lie at the bottom of our figure. Moreover, as expected, QCs decay with the increase of noise. Therefore, a hierarchy in QCs observed in Fig. 12 is in a good agreement with the quantum advantage obtained for the QI process, thereby connecting the inherent property of the quantum states with the illumination.

Interestingly, unlike most other quantum information protocols, it is not clear whether the entanglement content of the state leads to the quantum advantage in QI. In particular, we know that for QI with the TMSV state, in the limit of large signal strength, the quantum advantage vanishes [49], although the entanglement content, E , of the pure state quantified by the von-Neumann entropy of local mode (entanglement entropy), diverges. We now check how the normalized version, E/N_S , behave under the large N_S limit. For the TMSV state, $|\psi_r\rangle$, we know

$$E(|\psi_r\rangle) = \cosh^2 r \log \cosh^2 r - \sinh^2 r \log \sinh^2 r, \quad (30)$$

Since $N_S(|\psi_r\rangle) = \sinh^2 r$, entanglement reduces to

$$E = (N_S + 1) \log(N_S + 1) - N_S \log N_S. \quad (31)$$

Moreover, using Eq. (30), we have

$$\lim_{N_S \rightarrow \infty} \frac{E}{N_S} = \lim_{r \rightarrow \infty} \coth^2 r \log \cosh^2 r - \log \sinh^2 r = 0. \quad (32)$$

We know that for a given N_S , the TMSV provides the maximal entanglement since its reduced subsystems are thermal. Recall, the thermal states are the ones that yield the maximum entropy for a given temperature (average number of photons), and, therefore, for a fixed signal strength, the entanglement entropy content of the TMSV state is maximal among all other pure states. For any other state with a given value of N_S , the entanglement content, E' satisfies

$$E' < (N_S + 1) \log(N_S + 1) - N_S \log N_S = E. \quad (33)$$

Consequently, from Eq. (32), we can see that in the asymptotic limit,

$$\lim_{N_S \rightarrow \infty} \frac{E'}{N_S} = 0. \quad (34)$$

Physically, N_S value is highly dependent on the reflectivity, κ , and the number of copies, M used in QI. For example, in the case of the TMSV, $N_S = 1$ can be considered large for $M = 1000$ and $\kappa = 0.1$, while for the same value of κ but $M = 1$, N_S have to be taken to much higher value than unity to be considered as “large.”

Nevertheless, we clearly observe that unlike entanglement, the normalized version of it provides consistent results in the asymptotic case as well, and for large signal strengths, it clearly predicts vanishing quantum advantage for any state considered for QI. When one couples this fact with its accurate predictions of hierarchies of states based on the scale of quantum advantage, the normalized version of correlations make a strong case for themselves on having a deep connection with the quantum advantage obtained in the QI protocol.

VI. CONCLUSION

By exploiting the “weird” features of quantum mechanics, especially quantum correlations in the joint system, it was demonstrated that the performance in the detection of a weakly reflecting target immersed in a noisy environment can be improved, and was named as quantum illumination (QI). It is in some sense the quantum version of the radar. Since its inception, theoretical studies have come a long way and several efforts have been made to identify regimes for efficient implementation of the theory in order to achieve maximal quantum advantage. Several experiments have also been performed both in optical and microwave regimes exhibiting quantum advantage in illumination.

One of the most recent endeavors in the theoretical front is to use non-Gaussian states for quantum illumination. Since non-Gaussian states possess a high amount of quantum correlations, thereby becoming useful in several quantum information processing tasks which Gaussian counterparts fail to do, such an extension is natural. In our work, the non-Gaussian

states are obtained by adding or subtracting photons from the two-mode squeezed vacuum state, an efficient mechanism to generate non-Gaussian states experimentally. Our aim was to categorize non-Gaussian states based on their performance in quantum illumination which, in turn, reduces to the discrimination of two states.

Motivated from the study of entanglement in continuous variable systems, one of the ways in which the performance of the photon-added and -subtracted states can be analyzed is by comparing the Chernoff bound of non-Gaussian states with the Chernoff bound offered by the two-mode squeezed vacuum (TMSV) state from which they are obtained. Based on such comparison, the non-Gaussian states ubiquitously provide better performance, both in presence and absence of noise. On the other hand, a suitable quantity to quantify quantum advantage in QI is to compare Chernoff bounds between the given state and the coherent state having an equal signal intensity. In particular, it is defined as the difference between the Chernoff bounds of the coherent state and the given state under consideration for a fixed signal strength. Among the considered non-Gaussian states, photon-subtracted states from both the modes and states with photons added only in the idler mode (equivalently, subtraction of photons performed in the signal mode) turned out to be beneficial for obtaining quantum advantage in QI in absence of noise.

In any experimental implementation, noise is inevitable, and in our work, effects of different noisy probe states generated via different imperfections on the illumination procedure are investigated. Considering local noise, modeled by Gaussian distributions, we found that if the signal transmission line equally affects both the non-Gaussian and coherent states having equal signal strength, unlike a noiseless scenario, all non-Gaussian states give quantum advantage. Specifically, in presence of certain critical noise values, benefits via non-Gaussian states increase with the increase of noise. In addition, we considered faulty twin beam generators producing two-mode squeezed states having lower squeezing strength than the promised one, as well as imperfect photon addition and subtraction mechanisms. In all these situations, photon-subtraction in both the modes and in the signal mode always

give improvements in QI.

The final aspect that we discussed involves inefficiencies in the apparatus required in the photon addition and subtraction protocol. One of the principal issues is that the desired non-Gaussian states cannot be produced deterministically. Instead, we obtain the same only with some limited probability, while rest of the time, the states which we obtain are unusable. In such a situation, we derived the minimum efficiency required by the machine so that the probabilistic non-Gaussian states still outperforms the protocol with the TMSV state. We showed that, as the states incorporate more and more non-Gaussianity, the required efficiency of the machine decreases. Thus, we provided an effective routine to use the available resources in order to construct a better detection protocol. All these results demonstrating superiority of quantum states in the illumination process are also shown to be connected with the correlations present in the probe states.

We believe that our analysis provides a consistent way to analyze quantum illumination with non-Gaussian states, especially when imperfections are affecting the process. Moreover, our work provides an appropriate platform for classifying Gaussian and non-Gaussian states based on their performance in quantum illumination.

VII. ACKNOWLEDGEMENT

RG, SR, and ASD acknowledge the support from Interdisciplinary Cyber Physical Systems (ICPS) program of the Department of Science and Technology (DST), India, Grant No.: DST/ICPS/QuST/Theme- 1/2019/23. TD acknowledges support by Foundation for Polish Science (FNP), IRAP project ICTQT, contract no. 2018/MAB/5, co-financed by EU Smart Growth Operational Programme. We acknowledge the uses of *Armadillo* – a high quality linear algebra library for the C++ language [121, 122], *QIClib* – a modern C++ library for general purpose quantum information processing and quantum computing [123] and cluster computing facility at Harish-Chandra Research Institute.

-
- [1] R. Feynman, *Int J Theor Phys* **21**, 467 (1982).
 - [2] D. DiVincenzo, *Science* **270**, 255 (1996).
 - [3] R. Raussendorf and H. J. Briegel, *Phys. Rev. Lett.* **86**, 5188 (2001).
 - [4] P. Walther, K. Resch, T. Rudolph, E. Schenck, H. Weinfurter, V. Vedral, M. Aspelmeyer, and A. Zeilinger, *Nature* **434**, 169 (2005).
 - [5] H. Briegel, D. Browne, W. Dur, R. Raussendorf, and M. den Nest, *Nature* **5**, 19 (2009).
 - [6] A. Sen(De) and U. Sen, *Physics News* **40**, 17 (2010).
 - [7] N. Gisin and R. Thew, *Nat. Photon.* **1**, 165 (2007).
 - [8] R. Demkowicz-Dobrzański, A. Sen(De), U. Sen, and M. Lewenstein, *Phys. Rev. A* **80**, 012311 (2009).
 - [9] A. Sen(De), U. Sen, and M. Żukowski, *Phys. Rev. A* **68**, 032309 (2003).
 - [10] M. Hillery, V. Bužek, and A. Berthiaume, *Phys. Rev. A* **59**, 1829 (1999).
 - [11] R. Cleve, D. Gottesman, and H.-K. Lo, *Phys. Rev. Lett.* **83**, 648 (1999).
 - [12] A. Karlsson, M. Koashi, and N. Imoto, *Phys. Rev. A* **59**, 162 (1999).
 - [13] G. Spedalieri, C. Lupo, S. Braunstein, and S. Pirandola, *Quantum Science and Technology* **4**, 015008 (2018).
 - [14] C. H. Bennett, G. Brassard, C. Crépeau, R. Jozsa, A. Peres, and W. K. Wootters, *Phys. Rev. Lett.* **70**, 1895 (1993).
 - [15] D. Boschi, S. Branca, F. De Martini, L. Hardy, and S. Popescu, *Phys. Rev. Lett.* **80**, 1121 (1998).
 - [16] S. Pirandola, J. Eisert, C. Weedbrook, A. Furusawa, and S. L. Braunstein, *Nat. Phot.* **9**, 641 (2015).
 - [17] M. Horodecki, P. Horodecki, and R. Horodecki, *Phys. Rev. A* **60**, 1888 (1999).

- [18] E. O. Kiktenko, A. A. Popov, and A. K. Fedorov, *Phys. Rev. A* **93**, 062305 (2016).
- [19] C. Seida, A. El Allati, N. Metwally, and Y. Hassouni, *Modern Physics Letters A* **35**, 2050272 (2020).
- [20] P. Badziag, M. Horodecki, P. Horodecki, and R. Horodecki, *Phys. Rev. A* **62**, 012311 (2000).
- [21] F. Verstraete and H. Verschelde, *Phys. Rev. Lett.* **90**, 097901 (2009).
- [22] C. H. Bennett and S. J. Wiesner, *Phys. Rev. Lett.* **69**, 2881 (1992).
- [23] K. Mattle, H. Weinfurter, P. G. Kwiat, and A. Zeilinger, *Phys. Rev. Lett.* **76**, 4656 (1996).
- [24] D. Bruß, M. Lewenstein, A. Sen(De), U. Sen, D. G. M., and C. Macchiavello, *International Journal of Quantum Information* **4**, 415 (2006).
- [25] D. Bruß, G. M. D'Ariano, M. Lewenstein, C. Macchiavello, A. Sen(De), and U. Sen, *Phys. Rev. Lett.* **93**, 210501 (2014).
- [26] M. Horodecki and M. Piani, *J. Phys. A: Mathematical and Theoretical* **45**, 105306 (2012).
- [27] A. Sen(De) and U. Sen, *Phys. Rev. A* **81**, 012308 (2010).
- [28] T. Das, R. Prabhu, A. Sen(De), and U. Sen, *Phys. Rev. A* **92**, 052330 (2015).
- [29] T. Das, R. Prabhu, A. Sen(De), and U. Sen, *Phys. Rev. A* **90**, 022319 (2014).
- [30] C. H. Bennett and G. Brassard, *Proceedings of IEEE International Conference on Computers, Systems and Signal Processing* **175**, 8 (1984).
- [31] A. K. Ekert, *Phys. Rev. Lett.* **67**, 661 (1991).
- [32] T. Jennewein, C. Simon, G. Weihs, H. Weinfurter, and A. Zeilinger, *Phys. Rev. Lett.* **84**, 4729 (2000).
- [33] N. Gisin, G. Ribordy, W. Tittel, and H. Zbinden, *Rev. Mod. Phys.* **74**, 145 (2002).
- [34] V. Scarani, H. Bechmann-Pasquinucci, N. J. Cerf, M. Dušek, N. Lütkenhaus, and M. Peev, *Rev. Mod. Phys.* **81**, 1301 (2009).
- [35] P. Shor, in *Proceed. 35th Ann. Symp. on Found. of Com. Sc.* (1994) pp. 124–134.
- [36] *Proceedings of the Royal Society of London. Series A: Mathematical and Physical Sciences* **439**, 553 (1992).
- [37] L. K. Grover, in *28th ann. ACM symp. on Th. of comp. - STOC '96* (ACM Press, 1996).
- [38] E. Chitambar and G. Gour, *Rev. Mod. Phys.* **91**, 025001 (2019).
- [39] V. Giovannetti, S. Lloyd, and L. Maccone, *Science* **306**, 1330 (2004).
- [40] V. Giovannetti, S. Lloyd, and L. Maccone, *Phys. Rev. Lett.* **96**, 010401 (2006).
- [41] C. L. Degen, F. Reinhard, and P. Cappellaro, *Rev. Mod. Phys.* **89**, 035002 (2017).
- [42] V. Giovannetti, S. Lloyd, and L. Maccone, *Nat. Photon.* **5**, 222–229 (2011).
- [43] J. P. Dowling and K. P. Seshadreesan, *Journal of Lightwave Technology* **33**, 2359 (2015).
- [44] S.-H. Tan, B. I. Erkmen, V. Giovannetti, S. Guha, S. Lloyd, L. Maccone, S. Pirandola, and J. H. Shapiro, *Phys. Rev. Lett.* **101**, 253601 (2008).
- [45] Z. Zhang, S. Mouradian, F. N. C. Wong, and J. H. Shapiro, *Phys. Rev. Lett.* **114**, 110506 (2015).
- [46] J. Shapiro and S. Lloyd, *New Journal of Physics* **11**, 063045 (2009).
- [47] S. Lloyd, *Science* **321**, 1463 (2008).
- [48] J. H. Shapiro, *IEEE AESM* **35**, 8 (2020).
- [49] G. Sorelli, N. Treps, F. Grosshans, and F. Boust, arXiv:2005.07116.
- [50] G. De Palma and J. Borregaard, *Phys. Rev. A* **98**, 012101 (2018).
- [51] M. Sanz, U. Las Heras, J. J. García-Ripoll, E. Solano, and R. Di Candia, *Phys. Rev. Lett.* **118**, 070803 (2017).
- [52] S. Pirandola, B. Bardhan, T. Gehring, C. Weedbrook, and S. Lloyd, *Nat. Phot.* **12**, 724–733 (2018).
- [53] M. Lanzagorta, *Quantum Optics* **7727**, 7727K (2010).
- [54] M. Lanzagorta, *Synthesis Lectures on Quantum Computing* **3**, 1 (2011).
- [55] C. Chang, A. M. Vadiraj, J. Bourassa, B. Balaji, and C. M. Wilson, *Applied Physics Letters* **114** (2019), <https://doi.org/10.1063/1.5085002>.
- [56] M. M. Wilde, M. Tomamichel, S. Lloyd, and M. Berta, *Phys. Rev. Lett.* **119**, 120501 (2017).
- [57] A. Karsa, G. Spedalieri, Q. Zhuang, and S. Pirandola, *Phys. Rev. Research* **2**, 023414 (2020).
- [58] E. D. Lopaeva, I. Ruo Berchera, I. P. Degiovanni, S. Olivares, G. Brida, and M. Genovese, *Phys. Rev. Lett.* **110**, 153603 (2013).
- [59] Y. Jo, S. Lee, Y. Ihn, Z. Kim, and S.-Y. Lee, arXiv:2103.17006.
- [60] H. Yang, W. Roga, J. Pritchard, and J. Jeffers, *Optics Express* **29**, 8199 (2021).
- [61] M. F. Sacchi, *Phys. Rev. A* **72**, 014305 (2005).
- [62] Z. Zhang, M. Tengner, T. Zhong, F. N. C. Wong, and J. H. Shapiro, *Phys. Rev. Lett.* **111**, 010501 (2013).
- [63] S. Pirandola, *New Journal of Physics* **15**, 113046 (2013).
- [64] A. Karsa and S. Pirandola, *IEEE Aerospace and Electronic Systems Magazine* **35**, 22 (2020).
- [65] Y. Jo, S. Lee, Y. Ihn, Z. Kim, and S.-Y. Lee, *Phys. Rev. Research* **3**, 013006 (2021).
- [66] H. Yuen and J. Shapiro, *IEEE Transactions on Information Theory* **26**, 78 (1980).
- [67] E. D. Lopaeva, I. Ruo Berchera, I. P. Degiovanni, S. Olivares, G. Brida, and M. Genovese, *Phys. Rev. Lett.* **110**, 153603 (2013).
- [68] S. Guha and B. I. Erkmen, *Phys. Rev. A* **80**, 052310 (2009).
- [69] Q. Zhuang, Z. Zhang, and J. H. Shapiro, *Phys. Rev. Lett.* **118**, 040801 (2017).
- [70] D. G. England, B. Balaji, and B. J. Sussman, *Phys. Rev. A* **99**, 023828 (2019).
- [71] Q. Zhuang, Z. Zhang, and J. H. Shapiro, *Journal of the Optical Society of America B* **34**, 1567 (2017).
- [72] E. Flurin, N. Roch, F. Mallet, M. H. Devoret, and B. Huard, *Phys. Rev. Lett.* **109**, 183901 (2012).
- [73] H. Liu, D. Giovannini, H. He, D. England, B. Sussman, B. Balaji, and A. Helmy, *Optica* **6**, 1349 (2019).
- [74] P. P. Rohde and T. C. Ralph, *Journal of Modern Optics* **53**, 1589 (2006).
- [75] M. Bradshaw, S. M. Assad, J. Y. Haw, S.-H. Tan, P. K. Lam, and M. Gu, *Phys. Rev. A* **95**, 022333 (2017).
- [76] C. W., S. P., J. T., V. V., and M. G., *New Journal of Physics* **18**, 043027 (2016).
- [77] R. S., I. Berchera, I. Degiovanni, S. Olivares, M. Paris, G. Adesso, and M. Genovese, *Journal of the Optical Society of America B* **31**, 2045 (2014).
- [78] M. Bradshaw, S. M. Assad, J. Y. Haw, S.-H. Tan, P. K. Lam, and M. Gu, *Phys. Rev. A* **95**, 022333 (2017).
- [79] S. Ragy, I. R. Berchera, I. P. Degiovanni, S. Olivares, M. Paris, G. Adesso, and M. Genovese, *J. Opt. Soc. Am. B* **31**, 2045 (2014).
- [80] C. Weedbrook, S. Pirandola, J. Thompson, V. Vedral, and M. Gu, *New Journal of Physics* **18**, 043027 (2016).
- [81] L. Fan and M. S. Zubairy, *Phys. Rev. A* **98**, 012319 (2018).

- [82] S. Zhang, J. Guo, W. Bao, J. Shi, C. Jin, X. Zou, and G. Guo, *Phys. Rev. A* **89**, 062309 (2014).
- [83] S.-Y. Lee and H. Nha, *Phys. Rev. A* **82**, 053812 (2010).
- [84] S.-Y. Lee, S.-W. Ji, H.-J. Kim, and H. Nha, *Phys. Rev. A* **84**, 012302 (2011).
- [85] H. Chernoff, *The Annals of Mathematical Statistics* **23**, 493 (1952).
- [86] M. Nussbaum and A. Szkoła, *The Annals of Statistics* **37**, 1040 (2009).
- [87] S. L. Braunstein, *Phys. Rev. A* **42**, 474 (1990).
- [88] S. Pirandola and S. Lloyd, *Phys. Rev. A* **78**, 012331 (2008).
- [89] K. M. R. Audenaert, J. Calsamiglia, R. Muñoz Tapia, E. Bagan, L. Masanes, A. Acin, and F. Verstraete, *Phys. Rev. Lett.* **98**, 160501 (2007).
- [90] T. Kailath, *IEEE Transactions on Communication Technology* **15**, 52 (1967).
- [91] F. Nielsen, *IEEE Signal Processing Letters* **20**, 269 (2013).
- [92] C. Navarrete-Benlloch, R. García-Patrón, J. H. Shapiro, and N. J. Cerf, *Phys. Rev. A* **86**, 012328 (2012).
- [93] T. Das, R. Prabhu, A. Sen(De), and U. Sen, *Phys. Rev. A* **93**, 052313 (2016).
- [94] S. Roy, T. Chanda, T. Das, A. Sen(De), and U. Sen, *Phys. Rev. A* **98**, 052131 (2018).
- [95] M. Walschaers, Y.-S. Ra, and N. Treps, *Phys. Rev. A* **100**, 023828 (2019).
- [96] Y.-S. Ra, A. Dufour, M. Walschaers, C. Jacquard, T. Michel, C. Fabre, and N. Treps, *Nature Physics* **16**, 144 (2019).
- [97] S. M. Barnett and S. Croke, *Adv. Opt. Photon.* **1**, 238 (2009).
- [98] J. Calsamiglia, J. I. de Vicente, R. Muñoz Tapia, and E. Bagan, *Phys. Rev. Lett.* **105**, 080504 (2010).
- [99] C. A. Fuchs and J. van de Graaf, *IEEE Trans. Inf. Theor.* **45**, 1216–1227 (2006).
- [100] P. Marian and T. A. Marian, *Phys. Rev. A* **86**, 022340 (2012).
- [101] J. Calsamiglia, R. Muñoz Tapia, L. Masanes, A. Acin, and E. Bagan, *Phys. Rev. A* **77**, 032311 (2008).
- [102] K. M. R. Audenaert, M. Nussbaum, A. Szkoła, and F. Verstraete, *Communications in Mathematical Physics* **279**, 251 (2008).
- [103] M. Hayashi, *Phys. Rev. A* **76**, 062301 (2007).
- [104] K. Li, *The Annals of Statistics* **42**, 171 (2014).
- [105] G. Spedalieri and S. L. Braunstein, *Phys. Rev. A* **90**, 052307 (2014).
- [106] L. Rigovacca, A. Farace, A. De Pasquale, and V. Giovannetti, *Phys. Rev. A* **92**, 042331 (2015).
- [107] C. Helstrom, *Journal of Statistical Physics* **1**, 231 (1969).
- [108] C. W. Helstrom, *Journal of Statistical Physics* **1**, 231 (1969).
- [109] J. Shapiro and S. Lloyd, *New Journal of Physics* **11**, 063045 (2009).
- [110] M. Abramowitz and I. A. Stegun, “Handbook of mathematical functions, with formulas, graphs, and mathematical tables,” (Dover, 1972) pp. 576–579.
- [111] Y. Kang, H. X. Lu, Y.-H. Lo, D. S. Bethune, and W. P. Risk, *Applied Physics Letters* **83**, 2955 (2003).
- [112] S. Chen, L. You, W. Zhang, X. Yang, H. Li, L. Zhang, Z. Wang, and X. Xie, *Opt. Express* **23**, 10786 (2015).
- [113] H. Meyer, arXiv:0805.0771.
- [114] M. Kim and M. Bellini, *SPIE* (2008).
- [115] M. Bradshaw, L. O. Conlon, S. Tserkis, M. Gu, P. K. Lam, and S. M. Assad, *Phys. Rev. A* **103**, 062413 (2021).
- [116] W. Zurek, *Ann. Phys* **9**, 855 (2000).
- [117] W. H. Ollivier, H. and Zurek, *Phys. Rev. Lett.* **88**, 017901 (2001).
- [118] L. Henderson and V. Vedral, *Journal of Physics A: Mathematical and General* **34**, 6899 (2001).
- [119] G. Vidal and R. F. Werner, *Phys. Rev. A* **65**, 032314 (2002).
- [120] M. B. Plenio, *Phys. Rev. Lett.* **95**, 090503 (2005).
- [121] C. Sanderson and R. Curtin, *Journal of Open Source Software* **1**, 26 (2016).
- [122] C. Sanderson and R. Curtin, *Lecture Notes in Computer Science (LNCS)* **10931**, 422 (2018).
- [123] QIClib, <https://titaschanda.github.io/QIClib> .